3-D FEM/BEM-Hybrid Approach Based on a General Formulation of Huygens' Principle for Planar Layered Media

Thomas F. Eibert and Volkert Hansen, *Member, IEEE*

***Abstract*— Huygens' principle is used to exclude inhomogeneous regions and ideal conducting regions from planar layered structures. The fields in the inhomogeneous regions are modeled by the finite-element method (FEM) with tetrahedral edge elements in terms of the electric-field strength $\vec{E}$. The fields in the layered structure are described by an integral representation of the electric-field strength $\vec{E}$ in terms of equivalent electric and magnetic Huygens' surface current densities for the inhomogeneous regions, and in terms of electric Huygens' surface current densities for ideal conducting regions. It is formulated with the help of electromagnetic (EM) potentials resulting in low-order singular integral kernels to facilitate the numerical handling of the integral representation. A general formulation of the integral representation is given for observation points lying in the Huygens' surface. As compared to the homogeneous-space case, additional terms in the integral representation have to be considered if parts of the Huygens' surface lie in an interface of layers with different material properties. An integral equation is formulated and discretized by a Galerkin testing procedure [boundary-element method (BEM)], together with the finite-element (FE) system resulting in an unequivocal discretized description of the entire field problem. The method is validated with the help of a canonical test problem. Further numerical results are presented for dielectric resonators coupled to microstrip circuits.**

***Index Terms*— Boundary-element method (BEM), finite-element method (FEM), Huygens' principle, planar layered medium.**

I. Introduction

THE mathematical formulation of Huygens' principle allows the calculation of electromagnetic (EM) fields in a closed domain in terms of the tangential-field components on the boundary of the domain and with the help of the Green's functions of the domain [1]. This fact can be applied to separate complicated field problems into several less complicated parts, which are connected by the boundary conditions on the Huygens' surfaces. The crucial point is that after introducing the equivalent Huygens' sources, the regions exterior to the domain in which the Huygens' integral representation is applied are free of any fields and, therefore, can be filled with arbitrary materials. So, in many cases, solution domains can be constructed for which the Green's functions are known. This concept is widely used in surface integral equation techniques where ideal conducting objects or dielectric objects in free space are replaced by equivalent Huygens' sources on a surface enclosing these objects. After introducing the Huygens' sources, the integral equation can be formulated based on the free-space Green's function [2], [3]. If the excluded dielectric objects are homogeneous, the interior regions can be described by an integral formulation with a free-space Green's function also. If the dielectric bodies are inhomogeneous, they can effectively be modeled by a local field calculation technique like the finite-difference (FD) method or FEM. Practical implementations of such hybrid approaches which have been published since the 1970's are usually working with the finite-element method (FEM) due to its modeling flexibility [4]–[11]. A severe drawback of such FEM/boundary-element method (BEM) hybrid approaches is that the BEM part results in fully populated matrices often making the method computationally intensive as compared to a local method like FEM or the finite-difference time-domain (FDTD) method combined with a local absorbing boundary condition, resulting in a pure sparse system matrix [7], [12]–[14]. Therefore, hybrid methods in free space are mainly applied if one has a problem with some kind of symmetry (bodies of revolution [9]) or advanced properties of the hybrid method in dealing with several scattering objects or difficulty in dealing with ideal conducting antenna structures can be utilized [11].

The situation is quite different if we consider field calculations in planar layered media, which can be used as a model for a great class of practical problems (planar circuits, geophysical applications, hyperthermia, etc.). Here, in many cases, it is very difficult for pure local methods to give a satisfactory description of the solution domain (very thin layers, very thick layers, etc.). Most field calculation techniques for layered media are based on integral formulations involving Green's functions. Research interest in this subject started with the work of Sommerfeld in 1909 [15], [16] dealing with the exact solution for the EM field of an electric Hertzian dipole on a lossy dielectric half-space. The development of analytical representations for the Green's functions of the layered medium by use of so-called Sommerfeld integrals [17], [18] gave rise to the formulation of the first integral equation techniques. Until now, due to the complexity of such formulations, they are mostly restricted to the calculation of planar circuits within the layered medium [19]–[22]. In [23], a two-dimensional (2-D) method is presented, combining an

Manuscript received August 28, 1996; revised January 23, 1997.

The authors are with Lehrstuhl für Theoretische Elektrotechnik, Bergische Universität, 42119 Wuppertal, Germany.

Publisher Item Identifier S 0018-9480(97)04462-1.

integral equation formulation for homogeneous regions with an integral equation formulation of the layered medium, allowing field calculations in layered media with homogeneous finite-sized disturbations. The first FEM/BEM-hybrid techniques for planar layered media were suggested in [24], [25] for the 2-D case, and in [26] for the three-dimensional (3-D) case. A more complete description of the method in [26] was given in [27].

In this paper, the authors present a 3-D hybrid approach combining the FEM for anisotropic media with a surface integral equation formulation of the layered medium (i.e., BEM). First the model of the field problem is defined. Then the FEM is summarized. The BEM is developed starting with an integral representation of the electric-field strength $\vec{E}$ in the layered medium based on Huygens' principle. The integral representation formulated with EM potentials is analyzed for observation points in the Huygens' surface. It is found that in this case, the integral representation has to be modified if parts of the Huygens' surface lie in an interface between layers with different material properties. This is due to the fact that the singular character of the Green's functions in the layer interface is changed as compared to the homogeneous space case. The modified integral representation is used for the formulation of a mixed potential integral equation (MPIE), which is discretized by the method of moments (MoM). Numerical results for a canonical test problem and for the coupling of dielectric resonators to microstrip circuits are presented.

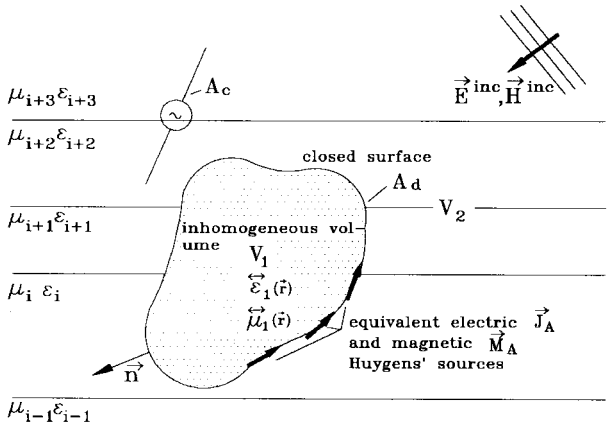

Fig. 1. Model of the field problem.

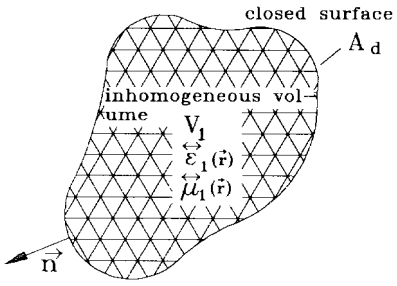

Fig. 2. FE model of the inhomogeneous region.

II. Formulation

A. Modeling the Field Problem

The field problem is considered for a suppressed time factor $e^{j\omega t}$. Applying Huygens' principle [1], the entire solution domain is separated into an inhomogeneous volume V_1, ideal conducting objects, and the remaining homogeneous planar layered medium designated by V_2 according to Fig. 1. V_1 and the ideal conducting objects can consist of several parts not connected to each other. The EM fields in V_1 are modeled by the FEM allowing nearly arbitrary inhomogeneous material distributions within this part of the solution domain. The volume V_1 is completely enclosed by the Huygens' surface A_d. Ideal conducting objects are enclosed by the Huygens' surface A_c. $A_c \cup A_d$ is designated as A. The fields in V_2 are modeled by a surface integral representation of the electric-field strength $\vec{E}$ in terms of equivalent electric and magnetic Huygens' surface currents on A_d and electric Huygens' surface currents on A_c. After introducing the equivalent Huygens' sources for the field representation in V_2, the regions exterior to V_2 are free of any fields and, therefore, can be filled with arbitrary materials. In this paper's case, materials are selected which are necessary to obtain an undistorted planar layered structure. So, for the integral representation of the fields in V_2, one can use the Green's functions of the undistorted layered medium. The integral representation in V_2 is transformed into an integral equation relating the Huygens' surface currents to each other. The integral equation is discretized by a BEM based on a Galerkin testing procedure.

The coupling of the FEM model of V_1 and the BEM description in V_2 is given by the boundary conditions on A_d

$$\vec{n}(\vec{r}) \times \vec{E}_1(\vec{r}) = \vec{n}(\vec{r}) \times \vec{E}_2(\vec{r}) \tag{1}$$

$$\vec{n}(\vec{r}) \times \vec{H}_1(\vec{r}) = \vec{n}(\vec{r}) \times \vec{H}_2(\vec{r}). \tag{2}$$

The boundary condition on A_c (ideal conducting) is

$$\vec{n}(\vec{r}) \times \vec{E}(\vec{r}) = 0. \tag{3}$$

$\vec{n}$ is the outward normal on A.

Both the FEM and the BEM result in coupled linear algebraic systems of equations, which are solved in a manner described in [11].

B. Finite-Element Method

The FEM is applied to the region V_1 in terms of the electric-field strength $\vec{E}$ according to Fig. 2. A weak formulation of the field problem can be obtained by the functional

$$F(\vec{E}_a, \vec{E}) = \iiint_{V_1} [(\nabla \times \vec{E}_a(\vec{r})) \cdot \overleftrightarrow{\mu}_r^{-1}(\vec{r}) \cdot (\nabla \times \vec{E}(\vec{r})) - k_0^2 \vec{E}_a(\vec{r}) \cdot \overleftrightarrow{\varepsilon}_r(\vec{r}) \cdot \vec{E}(\vec{r}) + jk_0 Z_0 \vec{E}_a(\vec{r}) \cdot \vec{J}_d(\vec{r})]\, dv + jk_0 Z_0 \oiint_{A_d} \vec{E}_a(\vec{r}) \cdot (\vec{H}(\vec{r}) \times \vec{n}(\vec{r}))\, da \tag{4}$$

which is stationary for the solution $\vec{E}$ of the field problem as well as for the solution $\vec{E}_a$ of the adjoint field problem [28]–[30]. k_0 and Z_0 are the wavenumber and the characteristic impedance of free space, respectively. $\vec{J}_d$ is a

possibly existing impressed current density. The functional is discretized by subdomain expansion functions on tetrahedral meshes

$$\vec{E}(\vec{r}) = \sum_{n=1}^{N} U_n \vec{\alpha}_n(\vec{r}) \tag{5}$$

$$\vec{E}_a(\vec{r}) = \sum_{n=1}^{N} U_n^a \vec{\alpha}_n(\vec{r}) \tag{6}$$

$$\vec{H}(\vec{r}) = \sum_{n=1}^{N} I_n \vec{\alpha}_n(\vec{r}). \tag{7}$$

$\vec{\alpha}_n$ are edge elements (Whitney edge elements), which are given by

$$\vec{\alpha}_n(\vec{r}) = \vec{w}_{ij}(\vec{r}) = \lambda_i \nabla \lambda_j - \lambda_j \nabla \lambda_i. \tag{8}$$

i, j are nodes of the tetrahedrons and λ_i, λ_j are the barycentric functions on the tetrahedrons. The fields modeled by these expansion functions are free of spurious modes (nonphysical solutions with nonvanishing divergence), because they only impose the continuity of the tangential-field components between adjacent tetrahedrons. Enforcing the stationary state of the functional with respect to the solution of the adjoint field solution, after substituting the expansion functions, results in a linear algebraic system of equations

$$\begin{aligned}[S_{mn}][U_n] - k_0^2[T_{mn}][U_n] + jk_0 Z_0[U_{mn}][I_n] \\ = -jk_0 Z_0[V_m], \qquad n,m = 1,\cdots,N\end{aligned} \tag{9}$$

with

$$[S]_{mn} = \iiint_{V_1} (\nabla \times \vec{\alpha}_n(\vec{r})) \cdot \overleftrightarrow{\mu}_r^{-1} \cdot (\nabla \times \vec{\alpha}_m(\vec{r}))\, dv \tag{10}$$

$$[T]_{mn} = \iiint_{V_1} \vec{\alpha}_m(\vec{r}) \cdot \overleftrightarrow{\varepsilon}_r \cdot \vec{\alpha}_n(\vec{r})\, dv \tag{11}$$

$$[U]_{mn} = \oiint_{A_d} \vec{\alpha}_m(\vec{r}) \cdot (\vec{\alpha}_n(\vec{r}) \times \vec{n}(\vec{r}))\, da \tag{12}$$

$$[V]_m = \iiint_{V_1} \vec{\alpha}_m(\vec{r}) \cdot \vec{J}_d(\vec{r})\, dv. \tag{13}$$

The matrix elements can be evaluated analytically with the help of [31] and taking into account the tensor forms of the anisotropic materials.

C. Boundary-Element Method

In Fig. 3, the field problem is illustrated as it is treated in the BEM. The electric-field strength $\vec{E}$ in V_2 is described by an integral representation in terms of the Huygens' surface current densities $\vec{J}_A$ and $\vec{M}_A$ on A_d and A_c. These current densities are related to the tangential components of the field strengths by

$$\begin{aligned}\vec{J}_A(\vec{r}) &= \vec{n}(\vec{r}) \times \vec{H}(\vec{r}) \\ \vec{M}_A(\vec{r}) &= -\vec{n}(\vec{r}) \times \vec{E}(\vec{r}).\end{aligned} \tag{14}$$

Due to the boundary conditions on A_d, these field strengths are directly coupled to the fields in V_1. For ideal conducting

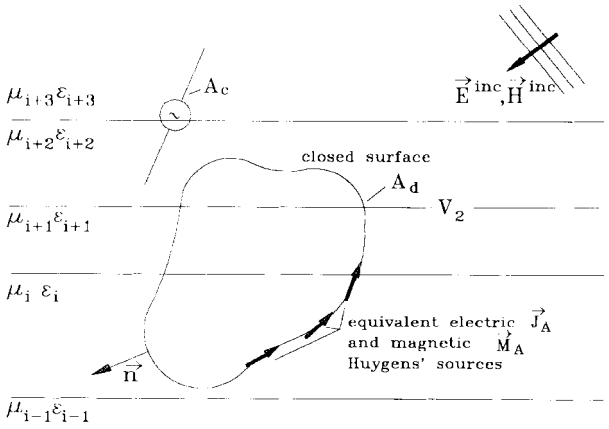

Fig. 3. Model for the integral equation formulation.

objects in V_2 enclosed by A_c, $\vec{M}_A$ vanishes and $\vec{J}_A$ is equivalent to the physical surface current density.

After introducing the equivalent Huygens' current densities, the fields in V_1 and in the ideal conducting regions due to the integral representation vanish and, therefore, these regions can be filled with arbitrary materials. This makes it possible to use an integral representation based on the Green's function of an undistorted planar layered structure. To facilitate the numerical handling of this integral representation, a so-called mixed potential formulation is used:

$$\begin{aligned}\vec{E}^m(\vec{r}) = &-j\omega \iint_A \overleftrightarrow{G}^{A^{mi}}(\vec{r},\vec{r}') \cdot \vec{J}_A^i(\vec{r}')\, da' \\ &- \nabla \iint_A G^{\Phi^{mi}}(\vec{r},\vec{r}') \rho_A^i(\vec{r}')\, da' \\ &+ \iint_A \overleftrightarrow{G}_M^{E^{mi}}(\vec{r},\vec{r}') \cdot \vec{M}_A^i(\vec{r}')\, da' + \vec{E}^{\text{inc},m}(\vec{r}).\end{aligned} \tag{15}$$

The index i stands for the source layer and the index m stands for the observation layer. $\vec{E}^{\text{inc},m}$ is the electric-field strength of incident fields in the observation layer. $\overleftrightarrow{G}^{A^{mi}}(\vec{r},\vec{r}')$ is the dyadic Green's function of the magnetic vector potential $\vec{A}$, $G^{\Phi^{mi}}(\vec{r},\vec{r}')$ is the Green's function for the electric scalar potential, and $\overleftrightarrow{G}_M^{E^{mi}}(\vec{r},\vec{r}')$ is the dyadic Green's function of the electric-field strength $\vec{E}$ for excitation with magnetic currents.

For a derivation of this formulation, especially of appropriate Green's functions $\overleftrightarrow{G}^{A^{mi}}$ and $G^{\Phi^{mi}}$, see [16], [27], [32].

In order to formulate an integral equation, one has to consider (15) for observation points $\vec{r}$ on the Huygens' surface A (in the following, restricted to smooth Huygens' surfaces). However, this is not a severe restriction, because in the resulting BEM, piecewise-smooth Huygens' surfaces are obtained. Due to the testing procedure, the edges and corners of these Huygens' surfaces give no contributions within the BEM. It is further assumed that the medium is layered with respect to the z-coordinate.

In the case $\vec{r} = \vec{r}'$, the integral kernels become singular. The usual procedure to overcome this problem is to deform

the Huygens' surface in the vicinity of $\vec{r}$ in the form of a small hemisphere (as it is illustrated in Fig. 4) and to analytically evaluate the integral contributions of the hemisphere for a vanishing radius of the hemisphere. If the Huygens' surface lies in a homogeneous material, the result of this calculation is well known [2]. This result can be accounted for on the left-hand side (LHS) of (15), resulting in

$$\frac{1}{2}\vec{E}(\vec{r}) = -j\omega \iint_A \overleftrightarrow{G}^A(\vec{r},\vec{r}')\cdot\vec{J}_A(\vec{r}')da' - \nabla \iint_A G^\Phi(\vec{r},\vec{r}') \rho_A(\vec{r}')\,da' + \iint_A \overleftrightarrow{G}_M^E(\vec{r},\vec{r}')\cdot\vec{M}_A(\vec{r}')\,da' + \vec{E}^{\text{inc}}(\vec{r}), \qquad \vec{r}\in A \tag{16}$$

with all of the integrals to be evaluated in a Cauchy principal value sense. If the Huygens' surface is situated in an interface between two layers with different material properties, this result is no longer valid because the singular character of the Green's functions is changed as compared to the homogeneous material case. To obtain the correct result, we can calculate the hemispherical integral contributions for the quasi-static image sources of the Green's functions at the layer interface and consider this contribution together with the homogeneous material contribution. In a first step, the Huygens' sources is expressed in (16) by the associated field quantities. With $\nabla\times\vec{H}^i(\vec{r}) = j\omega\varepsilon\vec{E}^i(\vec{r})$, one obtains for source-free regions

$$\begin{aligned}\vec{n}(\vec{r})\cdot\vec{E}^i(\vec{r}) &= \frac{1}{j\omega\varepsilon_i}\vec{n}(\vec{r})\cdot(\nabla(\vec{r})\times\vec{H}^i(\vec{r})) \\ &= -\frac{1}{j\omega\varepsilon_i}\nabla\cdot(\vec{n}(\vec{r})\times\vec{H}^i(\vec{r})) \\ &= -\frac{1}{j\omega\varepsilon_i}\nabla_A\cdot\vec{J}_A^i(\vec{r}) = \frac{1}{\varepsilon_i}\rho_A^i(\vec{r})\end{aligned} \tag{17}$$

and, therefore,

$$\rho_A^i(\vec{r}) = \varepsilon_i(\vec{n}(\vec{r})\cdot\vec{E}^i(\vec{r})). \tag{18}$$

$\nabla_A\cdot$ is the surface divergence operator. Together with (14), one obtains

$$\begin{aligned}\frac{1}{2}\vec{E}^m(\vec{r}) = &-j\omega\iint_A \overleftrightarrow{G}^{A^{mi}}(\vec{r},\vec{r}')\cdot(\vec{n}'(\vec{r}')\times\vec{H}^i(\vec{r}'))\,da' \\ &-\nabla\iint_A G^{\Phi^{mi}}(\vec{r},\vec{r}')\varepsilon_i(\vec{n}'(\vec{r}')\cdot\vec{E}^i(\vec{r}'))\,da' \\ &-\iint_A \overleftrightarrow{G}_M^{E^{mi}}(\vec{r},\vec{r}')\cdot(\vec{n}'(\vec{r}')\times\vec{E}^i(\vec{r}'))\,da' \\ &+\vec{E}^{\text{inc},m}(\vec{r}).\end{aligned} \tag{19}$$

Without loss of generality, one considers the configuration in Fig. 5 with $\vec{r} = (0,0,0)$.

The hemispherical integral contribution of the magnetic vector potential vanishes due to its low-order singularity. The quasi-static image sources of the Green's functions can be obtained by asymptotically evaluating the Sommerfeld integral representations of the Green's function [17], [18], [32]. In this

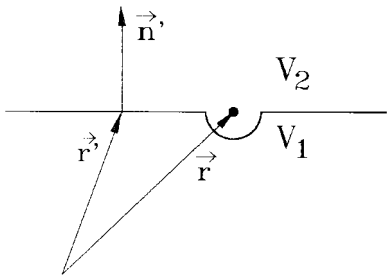

Fig. 4. Deformed Huygens' surface for $\vec{r} = \vec{r}'$.

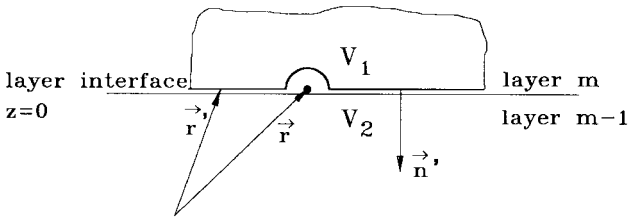

Fig. 5. Huygens' surface in the interface between two layers.

paper's case, $\overleftrightarrow{G}_M^E$ can be written as

$$\begin{aligned}\overleftrightarrow{G}_M^{E^{mm}}(\vec{0},\vec{r}') = &\frac{1}{4\pi}\frac{\varepsilon_{m-1}-\varepsilon_m}{\varepsilon_{m-1}+\varepsilon_m}\begin{pmatrix}0 & -\frac{z'}{2r'^3} & 0\\ \frac{z'}{2r'^3} & 0 & 0\\ \frac{y'}{r'^3} & -\frac{x'}{r'^3} & 0\end{pmatrix} \\ &+\frac{1}{4\pi}\frac{\mu_{m-1}-\mu_m}{\mu_{m-1}+\mu_m}\begin{pmatrix}0 & \frac{z'}{2r'^3} & -\frac{y'}{r'^3}\\ -\frac{z'}{2r'^3} & 0 & \frac{x'}{r'^3}\\ 0 & 0 & 0\end{pmatrix}\end{aligned} \tag{20}$$

where only terms giving a contribution to the hemispherical integral are considered. With

$$x' = r'\cos\varphi'\sin\vartheta' \tag{21}$$

$$y' = r'\sin\varphi'\sin\vartheta' \tag{22}$$

$$z' = r'\cos\vartheta' \tag{23}$$

$$\vec{n}'(\vec{r}') = -\vec{e}_{r'} = -\begin{pmatrix}\cos\varphi'\sin\vartheta'\\ \sin\varphi'\sin\vartheta'\\ \cos\vartheta'\end{pmatrix} \tag{24}$$

and

$$\vec{n}'(\vec{r}')\times\vec{E}(\vec{r}') = \begin{pmatrix}E_y(\vec{r}')\cos\vartheta' - E_z(\vec{r}')\sin\varphi'\sin\vartheta'\\ E_z(\vec{r}')\cos\varphi'\sin\vartheta' - E_x(\vec{r}')\cos\vartheta'\\ E_x(\vec{r}')\sin\varphi'\sin\vartheta' - E_y(\vec{r}')\cos\varphi'\sin\vartheta'\end{pmatrix} \tag{25}$$

one obtains

$$\begin{aligned}&-\iint_{A_0}\overleftrightarrow{G}_M^{E^{mm}}(\vec{r},\vec{r}')\cdot(\vec{n}'(\vec{r}')\times\vec{E}^m(\vec{r}'))\,da' \\ &=\frac{1}{4\pi}\frac{\varepsilon_{m-1}-\varepsilon_m}{\varepsilon_{m-1}+\varepsilon_m}\iint_{A_0}\begin{pmatrix}-\frac{1}{2}E_x^m(\vec{r}')\frac{\cos^2\vartheta'}{r'^2}\\ -\frac{1}{2}E_y^m(\vec{r}')\frac{\cos^2\vartheta'}{r'^2}\\ E_z^m(\vec{r}')\frac{\sin^2\vartheta'}{r'^2}\end{pmatrix}da' \\ &\quad+\frac{1}{4\pi}\frac{\mu_{m-1}-\mu_m}{\mu_{m-1}+\mu_m} \\ &\quad\times\iint_{A_0}\begin{pmatrix}+\frac{1}{2r'^2}E_x^m(\vec{r}')(\cos^2\vartheta'+\sin^2\vartheta')\\ +\frac{1}{2r'^2}E_y^m(\vec{r}')(\cos^2\vartheta'+\sin^2\vartheta')\\ 0\end{pmatrix}da'.\end{aligned} \tag{26}$$

A_0 is the integration domain of the hemisphere. The evaluation of the integrals is performed with the transformation

$$\iint\limits_{A_0} \cdots \quad da' = 2\pi \int_0^{\frac{\pi}{2}} \cdots \quad r'^2 \sin\vartheta' d\vartheta'. \tag{27}$$

Considering

$$\int_0^{\frac{\pi}{2}} \cos^2\vartheta' \sin\vartheta' d\vartheta' = \frac{1}{3} \tag{28}$$

$$\int_0^{\frac{\pi}{2}} \sin^3\vartheta' d\vartheta' = \frac{2}{3} \tag{29}$$

one finally obtains for vanishing r'

$$\begin{aligned} &-\iint\limits_{A_0} \overleftrightarrow{G}_M^{E^{mm}}(\vec{r},\vec{r}') \cdot (\vec{n}'(\vec{r}') \times \vec{E}^m(\vec{r}'))\, da' \\ &\quad = \frac{\varepsilon_{m-1}-\varepsilon_m}{\varepsilon_{m-1}+\varepsilon_m} \begin{pmatrix} -\frac{1}{12}E_x^m(\vec{0}) \\ -\frac{1}{12}E_y^m(\vec{0}) \\ \frac{1}{3}E_z^m(\vec{0}) \end{pmatrix} \\ &\qquad + \frac{\mu_{m-1}-\mu_m}{\mu_{m-1}+\mu_m} \begin{pmatrix} \frac{1}{4}E_x^m(\vec{0}) \\ \frac{1}{4}E_y^m(\vec{0}) \\ 0 \end{pmatrix}. \end{aligned} \tag{30}$$

For ∇G^{Φ}, one obtains

$$\nabla G^{\Phi^{mm}}(\vec{0},\vec{r}') = \frac{1}{4\pi\varepsilon_m} \frac{\varepsilon_{m-1}-\varepsilon_m}{\varepsilon_{m-1}+\varepsilon_m} \frac{1}{r'^3} \begin{pmatrix} -x' \\ -y' \\ z' \end{pmatrix}. \tag{31}$$

With

$$\begin{aligned} \vec{n}'(\vec{r}') \cdot \vec{E}(\vec{r}') = -(&\cos\varphi' \sin\vartheta' E_x(\vec{r}') + \sin\varphi' \sin\vartheta' E_y(\vec{r}') \\ &+ \cos\vartheta' E_z(\vec{r}')) \end{aligned} \tag{32}$$

one finds

$$\begin{aligned} &-\nabla \iint\limits_{A_0} \overleftrightarrow{G}^{\Phi^{mm}}(\vec{r},\vec{r}')\varepsilon_m(\vec{n}'(\vec{r}') \cdot \vec{E}^m(\vec{r}'))\, da' \\ &\quad = \frac{1}{4\pi} \frac{\varepsilon_{m-1}-\varepsilon_m}{\varepsilon_{m-1}+\varepsilon_m} \iint\limits_{A_0} \begin{pmatrix} -\frac{1}{2}E_x^m(\vec{r}')\frac{\sin^2\vartheta'}{r'^2} \\ -\frac{1}{2}E_y^m(\vec{r}')\frac{\sin^2\vartheta'}{r'^2} \\ E_z^m(\vec{r}')\frac{\cos^2\vartheta'}{r'^2} \end{pmatrix} da' \\ &\quad = \frac{\varepsilon_{m-1}-\varepsilon_m}{\varepsilon_{m-1}+\varepsilon_m} \begin{pmatrix} -\frac{1}{6}E_x^m(\vec{0}) \\ -\frac{1}{6}E_y^m(\vec{0}) \\ \frac{1}{6}E_z^m(\vec{0}) \end{pmatrix}. \end{aligned} \tag{33}$$

If V_1 is below the layer interface, the calculations can be performed analogously. In the result, the index $m-1$ has to be replaced by $m+1$. The results can be summarized to

$$\begin{aligned} &\frac{1}{2}\vec{E}^m(\vec{r}) + \left[\frac{1}{4}\frac{\varepsilon_{m\pm1}-\varepsilon_m}{\varepsilon_{m\pm1}+\varepsilon_m} \begin{pmatrix} E_x^m(\vec{r}) \\ E_y^m(\vec{r}) \\ -2E_z^m(\vec{r}) \end{pmatrix} \right. \\ &\quad \left. - \frac{1}{4}\frac{\mu_{m\pm1}-\mu_m}{\mu_{m\pm1}+\mu_m} \begin{pmatrix} E_x^m(\vec{r}) \\ E_y^m(\vec{r}) \\ 0 \end{pmatrix} \right] \delta_{z,\substack{d_{m+1} \\ d_m}} \\ &\quad = -j\omega \iint\limits_A \overleftrightarrow{G}^{A^{mi}}(\vec{r},\vec{r}') \cdot \vec{J}_A^i(\vec{r}')\, da' \\ &\qquad - \nabla \iint\limits_A \overleftrightarrow{G}^{\Phi^{mi}}(\vec{r},\vec{r}')\rho_A^i(\vec{r}')\, da' + \iint\limits_A \overleftrightarrow{G}_M^{E^{mi}}(\vec{r},\vec{r}') \\ &\qquad \cdot \vec{M}_A^i(\vec{r}')da' + \vec{E}^{\text{inc},m}(\vec{r}), \qquad \vec{r} \in A \end{aligned} \tag{34}$$

with

$$\delta_{z,d} = \begin{cases} 1, & z = d \\ 0, & z \neq d. \end{cases} \tag{35}$$

d_m is the z-coordinate of the interface between layer m and layer $m-1$.

Now an integral equation for the tangential-field components in A_c and A_d can be formulated.

$$\begin{aligned} &\vec{n}(\vec{r}) \times \left[\left(\frac{1}{2} + \frac{1}{4} \left\{ \frac{\varepsilon_{m\pm1}-\varepsilon_m}{\varepsilon_{m\pm1}+\varepsilon_m} \right. \right. \right. \\ &\qquad \left. \left. \left. - \frac{\mu_{m\pm1}-\mu_m}{\mu_{m\pm1}+\mu_m} \right\} \delta_{z,\substack{d_{m+1} \\ d_m}} \right) \vec{E}^m(\vec{r}) \right] \Bigg|_{\vec{r}\in A_d} \\ &\quad = \vec{n}(\vec{r}) \times \left[-j\omega \iint\limits_{A_c \cup A_d} \overleftrightarrow{G}^{A^{mi}}(\vec{r},\vec{r}') \cdot \vec{J}_A^i(\vec{r}')\, da' \right. \\ &\qquad - \nabla \iint\limits_{A_c \cup A_d} G^{\Phi^{mi}}(\vec{r},\vec{r}')\rho_A^i(\vec{r}')\, da' \\ &\qquad \left. + \iint\limits_{A_d} \overleftrightarrow{G}_M^{E^{mi}}(\vec{r},\vec{r}') \cdot \vec{M}_A^i(\vec{r}')\, da' + \vec{E}^{\text{inc},m}(\vec{r}) \right] \Bigg|_{\vec{r}\in A_d} \end{aligned} \tag{36}$$

$$\begin{aligned} 0 = \vec{n}(\vec{r}) \times \Bigg[&-j\omega \iint\limits_{A_c \cup A_d} \overleftrightarrow{G}^{A^{mi}}(\vec{r},\vec{r}') \cdot \vec{J}_A^i(\vec{r}')\, da' \\ &-\nabla \iint\limits_{A_c \cup A_d} G^{\Phi^{mi}}(\vec{r},\vec{r}')\rho_A^i(\vec{r}')\, da' + \iint\limits_{A_d} \overleftrightarrow{G}_M^{E^{mi}}(\vec{r},\vec{r}') \\ &\cdot \vec{M}_A^i(\vec{r}')\, da' + \vec{E}^{\text{inc},m}(\vec{r}) \Bigg] \Bigg|_{\vec{r}\in A_c} \end{aligned} \tag{37}$$

where the fact that the layer interfaces are parallel to the xy-plane have been utilized. The integral equation is discretized by vector expansion functions. Then the discretized equation is transformed into a linear algebraic system of equations based on a Galerkin testing procedure. With the help of some vector analytical transformations [3], one finally obtains

$$\begin{aligned} [A_{\text{ln}}][U_n] = -[B_{\text{ln}}][I_n] + [C_{\text{ln}}][I_n] - [D_{\text{ln}}][U_n] + [G_l], \\ l,n = 1,\cdots,N \end{aligned} \tag{38}$$

with

$$\begin{aligned} [A]_{\text{ln}} = &\iint\limits_{A_l} \left(\frac{1}{2} + \frac{1}{4} \left\{ \frac{\varepsilon_{m\pm1}-\varepsilon_m}{\varepsilon_{m\pm1}+\varepsilon_m} - \frac{\mu_{m\pm1}-\mu_m}{\mu_{m\pm1}+\mu_m} \right\} \right. \\ &\left. \times \delta_{z,\substack{d_{m+1} \\ d_m}} \right) \vec{\alpha}_n(\vec{r}) \cdot \vec{\beta}_l(\vec{r})\, da, \qquad A_l \subset A_d \\ &= 0, \qquad A_l \subset A_c, \end{aligned} \tag{39}$$

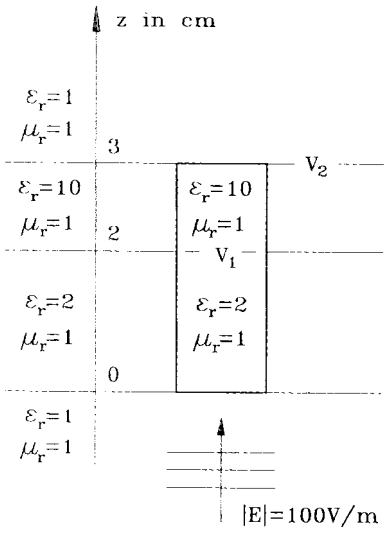

Fig. 6. Canonical test problem.

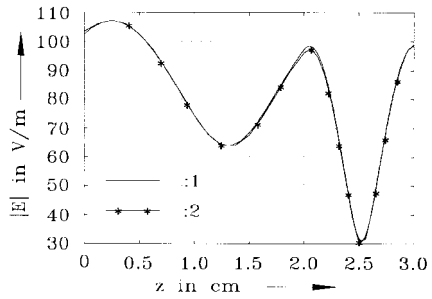

Fig. 7. $|E| = \sqrt{\vec{E} \cdot \vec{E}^*}$ along the axis of V_1, $f = 5$ GHz, 1: analytical result, 2: numerical result.

$$[B]_{ln} = j\omega \iint_{A_l} \vec{\beta}_l(\vec{r}) \cdot \iint_{A_n} \overleftrightarrow{G}^{A^{mi}}(\vec{r},\vec{r}') \cdot \vec{\beta}_n(\vec{r}')\, da'\, da \tag{40}$$

$$[C]_{ln} = -\frac{1}{j\omega} \iint_{A_l} \nabla_A \cdot \vec{\beta}_l(\vec{r}) \iint_{A_n} G^{\Phi^{mi}}(\vec{r},\vec{r}') \times \nabla_A \cdot \beta_n(\vec{r}')\, da'\, da \tag{41}$$

$$[D]_{ln} = \iint_{A_l} \vec{\beta}_l(\vec{r}) \cdot \iint_{A_n} \overleftrightarrow{G}_M^{E^{mi}}(\vec{r},\vec{r}') \cdot \vec{\beta}_n(\vec{r}')\, da'\, da, \quad A_n \subset A_d$$
$$= 0, \quad A_n \subset A_c \tag{42}$$

$$[G]_l = \iint_{A_l} \vec{\beta}_l(\vec{r}) \cdot \vec{E}^{\text{inc},m}(\vec{r})\, da \tag{43}$$

with $\vec{\beta}_n(\vec{r}) = \vec{n} \times \vec{\alpha}_n(\vec{r})$. The $\vec{\alpha}_n(\vec{r})$ are the tangential parts in the triangles on A_d of the edge element-expansion functions in the tetrahedrons of V_1. They are also used on A_c. The resulting $\vec{\beta}_n(\vec{r})$ are equivalent to the current expansion functions in [3]. A_n and A_l are the source and testing subdomains, respectively. The evaluation of the matrix elements is performed as described in [11], [27], [33]. Internal resonances of the integral equation formulation are effectively suppressed by the parasitic body technique [34], [35].

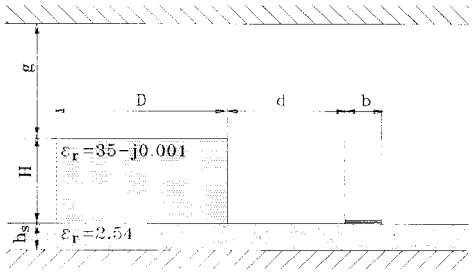

Fig. 8. Geometry of the dielectric resonator coupled to a microstrip line, $H = 7.5$ mm, $D = 14$ mm, $g = 11$ mm, $b = 2.25$ mm and $h_s = 0.8$ mm.

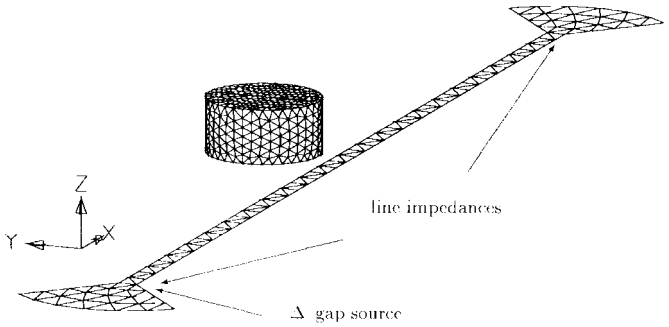

Fig. 9. FE model of the dielectric resonator coupled to a microstrip line.

III. Applications and Results

In a first example, the FEM/BEM-hybrid technique was applied to a canonical test problem for which the analytical result is known. A homogeneous plane wave propagating in the z-direction is incident on a layered structure consisting of four layers (as illustrated in Fig. 6). The material properties inside the cubical volume V_1, which extends over two layers, are equal to the material properties of the surrounding layers. Thus, the field solution of the plane wave in the undistorted layered structure has to be reproduced inside V_1 if the hybrid method is applied. A comparison of the analytical solution to the numerical results for the magnitude of the electric-field strength $\vec{E}$ (given in Fig. 7) shows excellent agreement between the two curves. If the additional terms of the generalized form of the integral equation are not considered, there are large errors—especially at the layer interfaces $z = 0$ cm and $z = 3$ cm, as can be expected due to the local behavior of these terms.

In a second example, the coupling of a cylindrical dielectric resonator operating in the $TE_{01\delta}$ mode to a microstrip line is considered. A cross-sectional view of the geometrical configuration is illustrated in Fig. 8. The FEM model of the field problem is shown in Fig. 9. The dielectric resonator is discretized with tetrahedral elements, and the ideal conducting microstrip line is modeled with triangular boundary elements in the BEM framework. It is excited by a Δ-gap voltage source. The 50-Ω microstrip line was ideally matched (dielectric resonator not present) with the help of the radial stubs and two line impedances. Due to the matching of the microstrip line, the S-parameters can easily be determined without de-embedding. $|S_{21}|$ curves for different distances between resonator and microstrip line are given in Fig. 10. In Fig. 11, the external quality factors of the resonator circuit

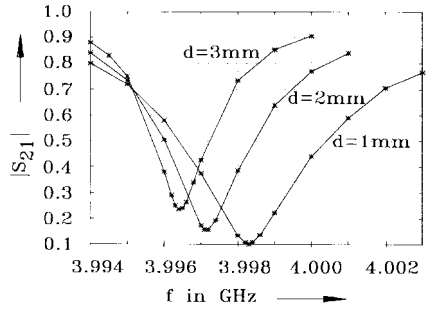

Fig. 10. $|S_{21}|$ resonance curves for the dielectric resonator/microstrip configuration in Fig. 9.

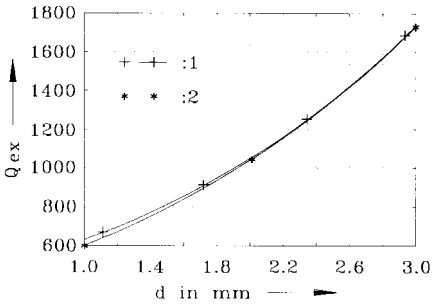

Fig. 11. External quality factor $Q_{\rm ex}$ of the dielectric resonator in Fig. 9. 1: numerical results. 2: measured results [36].

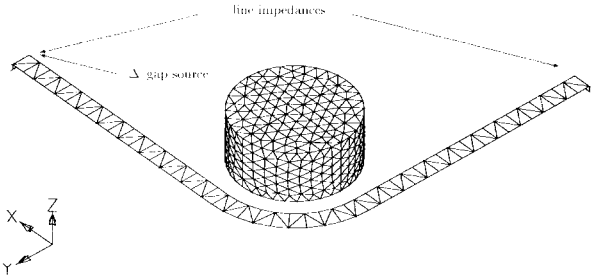

Fig. 12. FE model of the dielectric resonator coupled to a curved microstrip line.

are compared to the measured results of [36]. The external quality factors were determined with the help of the formulas in [37]. Agreement between measured and numerical results is very good. For reliable numerical results, the additional terms of the generalized integral equation formulation are, again, very important.

Finally, in a third example, the coupling of a dielectric resonator to a curved microstrip line was investigated. The finite-element (FE) model of the field problem is shown in Fig. 12. The measures and material properties of the substrate, the dielectric resonator, and the microstrip line are the same as in the second example (see Fig. 8). As opposed to the second example here, the 50-Ω microstrip line is matched by via-holes to the bottom reflector, together with line impedances at the via-holes (see Fig. 12). In this case, less boundary elements for the modeling of the matched microstrip line are needed. The configuration was calculated for several distances between the dielectric resonator and the microstrip line. The results can be seen in Figs. 13 and 14 with the quality factors

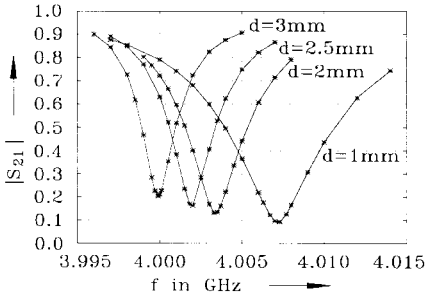

Fig. 13. $|S_{21}|$ resonance curves for the dielectric resonator/microstrip configuration in Fig. 12.

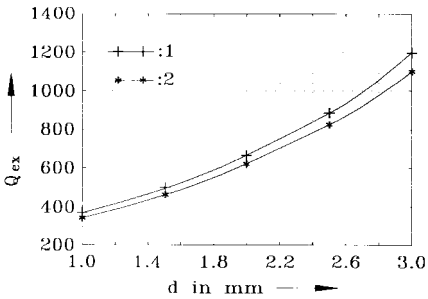

Fig. 14. External quality factor $Q_{\rm ex}$ of the dielectric resonator in Fig. 12. 1: numerical results. 2: measured results [36].

determined with the formulas in [37]. The curves in Fig. 14 show slightly higher differences between the calculated results and the measured results from [36] for the straight microstrip line. This might be due to the fact that no exact values for the radius of curvature of the curved microstrip line are given in [36].

IV. Conclusion

Based on Huygens' principle, a FEM/BEM-hybrid approach for planar layered media was formulated. Anisotropic inhomogeneous regions, as well as ideal conducting bodies, were excluded from the layered medium and replaced by equivalent electric and magnetic Huygens' surface currents. The inhomogeneous regions were modeled by the FEM with tetrahedral edge element meshes. The fields in the layered structure due to the Huygens' sources were described by a mixed potential integral representation for the electric-field strength based on the Green's functions of the layered medium. A general formulation of the integral representation was given, which is valid for observation points on the Huygens' surface even if the Huygens' surface lies in the interface between two layers. An integral equation was formulated and solved. Numerical results for a canonical test problem and the coupling of dielectric resonators to microstrip circuits were also presented.

References

[1] J. C. Monzon, "On surface integral representations: Validity of Huygen's principle and the equivalence principle in inhomogeneous bianisotropic media," *IEEE Trans. Microwave Theory Tech.*, vol. 41, pp. 1995–2001, Nov. 1993.

[2] R. Mittra, *Computer Techniques for Electromagnetics*. New York: Pergamon, 1973.

[3] S. M. Rao, D. R. Wilton, and A. W. Glisson, "Electromagnetic scattering by surfaces of arbitrary shape," *IEEE. Trans. Antennas Propagat.*, vol. AP-30, pp. 409–418, Mar. 1982.
[4] B. H. McDonald and A. Wexler, "Finite-element solution of unbounded field problems," *IEEE Trans. Microwave Theory Tech.*, vol. MTT-20, pp. 841–847, Dec. 1972.
[5] X. Yuan, "Three-dimensional electromagnetic scattering from inhomogeneous objects by the hybrid moment and finite element method," *IEEE Trans. Microwave Theory Tech.*, vol. 38, pp. 1053–1058, Aug. 1990.
[6] J.-J. Angelini, C. Soize, and P. Soudais, "Hybrid numerical method for harmonic 3-D maxwell equations: Scattering by a mixed conducting and inhomogeneous anisotropic dielectric medium," *IEEE. Trans. Antennas Propagat.*, vol. 41, pp. 66–76, Jan. 1993.
[7] J. Jin, *The Finite Element Method in Electromagnetics*. New York: Wiley, 1993.
[8] G. E. Antilla and N. G. Alexopoulos, "Scattering from complex three-dimensional geometries by a curvilinear hybrid finite-element-integral equation approach," *J. Opt. Soc. Amer. A, Opt. Image Sci.*, vol. 11, no. 4, pp. 1445–1456 (Errata, p. 3322, Dec. 1994).
[9] W. E. Boyse and A. A. Seidl, "A hybrid finite element method for 3-D scattering using nodal and edge elements," *IEEE. Trans. Antennas Propagat.*, vol. 42, pp. 1436–1442, Oct. 1994.
[10] J. L. Volakis, A. Chatterjee, and J. Gong, "A class of hybrid finite element methods for electromagnetics: A review," *J. Electromagn. Waves and Appl.*, vol. 8, no. 9/10, pp. 1095–1124, 1994.
[11] T. Eibert and V. Hansen, "Calculation of unbounded field problems in free space by a 3-D FEM/BEM-hybrid approach," *J. Electromagn. Waves and Appl.*, vol. 10, no. 1, pp. 61–78, 1996.
[12] K. S. Kunz and R. J. Luebbers, *The Finite Difference Time Domain Method for Electromagnetics*. Boca Raton, FL: CRC Press, 1993.
[13] D. Givoli, "Non-reflecting boundary conditions: Review article," *J. Comput. Phys.*, vol. 94, pp. 1–29, 1991.
[14] J.-P. Berenger, "A perfectly matched layer for the absorption of electromagnetic waves," *J. Comput. Phys.*, vol. 114, pp. 185–200, 1994.
[15] A. Sommerfeld, "Über die Ausbreitung der Wellen in der drahtlosen Telegraphie," *Ann. Phys.*, vol. 28, pp. 665–736, 1909.
[16] ———, *Partielle Differentialgleichungen der Physik*. Leipzig, Germany: Akademische Verlagsgesellschaft, 1962.
[17] L. B. Felsen and N. Marcuvitz, *Radiation and Scattering of Waves*, (Electromagnetic Waves Series). Piscataway, NJ: IEEE Press, 1994.
[18] V. W. Hansen, *Numerical Solution of Antennas in Layered Media*. New York: Wiley, 1989.
[19] J. R. Mosig, "Arbitrarily shaped microstrip structures and their analysis with a mixed potential integral equation," *IEEE Trans. Microwave Theory Tech.*, vol. 36, pp. 314–323, Feb. 1988.
[20] R. W. Jackson, "Full-wave, finite element analysis of irregular microstrip discontinuities," *IEEE Trans. Microwave Theory Tech.*, vol. 37, pp. 81–89, Jan. 1989.
[21] T.-S. Horng, W. E. McKinzie, and N. G. Alexopoulos, "Full-wave spectral-domain analysis of compensation of microstrip discontinuities using triangular subdomain functions," *IEEE Trans. Microwave Theory Tech.*, vol. 40, pp. 2137–2147, Dec. 1992.
[22] J. Sercu, N. Faché, F. Libbrecht, and P. Lagase, "Mixed potential integral equation technique for hybrid microstrip–slotline multilayered circuits using a mixed rectangular-triangular mesh," *IEEE Trans. Microwave Theory Tech.*, vol. 43, pp. 1162–1171, May 1995.
[23] F. Olyslager, D. De Zutter, and K. Blomme, "Rigorous analysis of the propagation characteristics of general lossless and lossy multiconductor transmission lines in multilayered media," *IEEE Trans. Microwave Theory Tech.*, vol. 41, pp. 79–88, Jan. 1993.
[24] I. Elshafiey, L. Udpa, and S. S. Udpa, "Scattering from two-dimensional objects embedded in multilayered media," *IEEE Trans. Magn.*, vol. 30, pp. 3160–3163, May 1994.
[25] J. Wu and K. A. Michalski, "Hybrid finite element—Mixed-potential integral equation—Discrete complex image approach for inhomogeneous waveguides in layered media," in *IEEE Antennas Propagat.-S Int. Symp.*, Newport Beach, CA, June 1995, pp. 1472–1475.
[26] T. F. Eibert and V. Hansen, "FEM/BEM-hybrid approach for layered media," in *IEEE Antennas Propagat.-S Int. Symp.*, Newport Beach, CA, June 1995, pp. 1464–1467.
[27] ———, "3-D FEM/BEM-hybrid approach for planar layered media," *Electromagnetics*, vol. 16, no. 3, pp. 253–272, May–June 1996.
[28] A. Konrad, "Vector variational formulation of electromagnetic fields in anisotropic media," *IEEE Trans. Microwave Theory Tech.*, vol. MTT-24, pp. 553–559, Sept. 1976.
[29] G. Jeng and A. Wexler, "Self-adjoint variational formulation of problems having nonself-adjoint operators," *IEEE Trans. Microwave Theory Tech.*, vol. MTT-26, pp. 91–94, Feb. 1978.
[30] W. Sun and C. A. Balanis, "Edge-based FEM solution of scattering from inhomogeneous and anisotropic objects," *IEEE Trans. Antennas Propagat.*, vol. 42, pp. 627–632, May 1994.
[31] J.-F. Lee and R. Mittra, "A note on the application of edge-elements for modeling three-dimensional inhomogeneously-filled cavities," *IEEE Trans. Microwave Theory Tech.*, vol. 40, pp. 1767–1773, Apr. 1992.
[32] K. A. Michalski and D. Zheng, "Electromagnetic scattering and radiation by surfaces of arbitrary shape in layered media, Part I: Theory," *IEEE Trans. Antennas Propagat.*, vol. 38, pp. 335–344, Mar. 1990.
[33] T. F. Eibert and V. Hansen, "On the calculation of potential integrals for linear source distributions on triangular domains," *IEEE Trans. Antennas Propagat.*, vol. 43, pp. 1499–1502, Dec. 1995.
[34] J. C. Monzon and N. J. Damaskos, "A scheme for eliminating internal resonances: The parasitic body technique," *IEEE. Trans. Antennas Propagat.*, vol. 42, pp. 1089–1096, Aug. 1994.
[35] T. F. Eibert and V. Hansen, "On the interior resonance problem of FEM/BEM-hybrid and BEM-approaches," in *IEEE Antennas Propagat.-S Int. Symp.*, Baltimore, MD, July 1996, pp. 154–157.
[36] P. Guillon, B. Byzery, and M. Chaubet, "Coupling parameters between a dielectric resonator and a microstripline," *IEEE Trans. Microwave Theory Tech.*, vol. MTT-33, pp. 222–226, Mar. 1985.
[37] A. Khanna and Y. Garault, "Determination of loaded, unloaded, and external quality factors of a dielectric resonator coupled to a microstrip line," *IEEE Trans. Microwave Theory Tech.*, vol. MTT-31, pp. 261–264, Mar. 1983.

Thomas F. Eibert was born on March 20, 1966 in Höchstadt, Germany. He received the Dipl.-Ing. (FH) degree in elektrotechnik from the Georg-Simon Ohm Fachhochhochschule in Nürnberg, Germany, in 1989, and the Dipl.-Ing. degree in elektrotechnik from the Ruhr-Universität Bochum, Germany in 1992. He is currently working toward the Dr.-Ing. degree at the Lehrstuhl für Theoretische Elektrotechnik, Bergische Universität–Gesamthochschule, Wuppertal, Germany.

From 1992 to 1994, he was with the Institut für Hochfrequenztechnik, Ruhr-Universität, Bochum, Germany. His primary research interests include EM-field calculations by hybrid methods combining local and global techniques and integral equation techniques for planar stratified media.

Volkert Hansen (M'82) received the Dipl.-Ing. degree in electrical engineering from the Technische Hochschule Darmstadt, Germany, in 1969. He received the Dr.-Ing. degree from the Institut für Hoch-und Höchstfrequenztechnik of the Ruhr-Universität, Bochum, Germany, in 1975.

He then joined the Institut für Hoch-und Höchstfrequenztechnik of the Ruhr-Universität, Bochum, Germany, as a Research Assistant. In 1985, he worked as a member of the electrical engineering faculty at Ruhr-Universität, and in 1990 he was appointed Professor. Since 1994, he has been a Full Professor of theoretical electrical engineering at the Bergische Universität-Gesamthochschule, Wuppertal, Germany. His main research interest is the development of theoretical and numerical methods for antennas and scattering problems with applications to planar circuits and antennas, focusing antennas, frequency and polarization selective screens, antennas for geophysical prospecting, and the evaluation of potential health effects of EM fields.

Dr. Hansen is a member of URSI Commision B, and ITG.